Electronic Supplementary Material (ESI) for New Journal of Chemistry.


# Phosphorus-nitrogen compounds. part 70. Syntheses of tetraaminomono/bis(4-fluorobenzyl)spiro(N/N)cyclotriphosphazenes: Structural characterizations and comparative evaluation of esterase activities of hCA I and hCA II isoenzymes

Aytuğ Okumuş[a,*], Gamze Elmas[a,*], Arzu Binici[b], Ekrem Tunca[c], Tuncer Hökelek[d] and Zeynel Kılıç[a]

[a] Department of Chemistry, Ankara University, 06100 Ankara, Türkiye

[b] Republic of Turkey, Ministry of Health, 06100 Ankara, Türkiye

[c] Department of Biochemistry, Dumlupınar University, 43100 Kütahya, Türkiye

[d] Department of Physics, Hacettepe University, 06800 Ankara, Türkiye

## Supporting Information

### Contents

**Section S1. All ESI-MS, NMR and FTIR spectra of 1a, 1b, 2a and 2b**

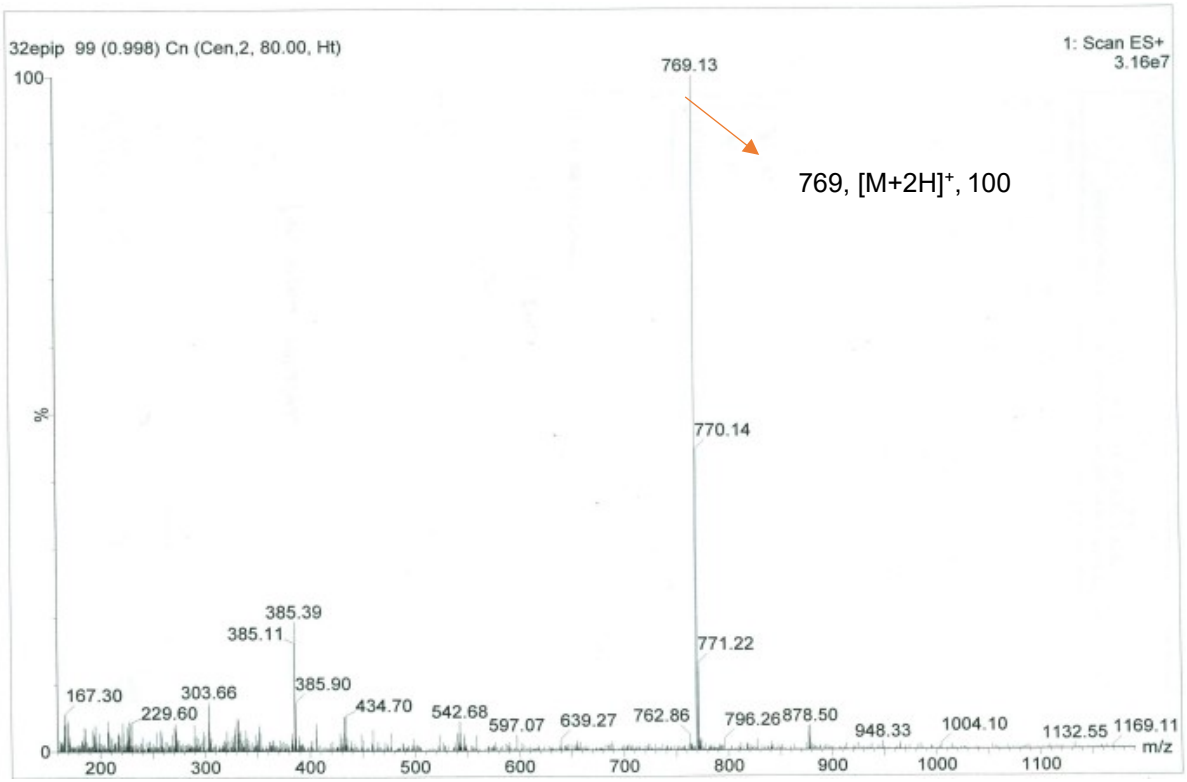


ESI-MS spectra of compounds **1a**.

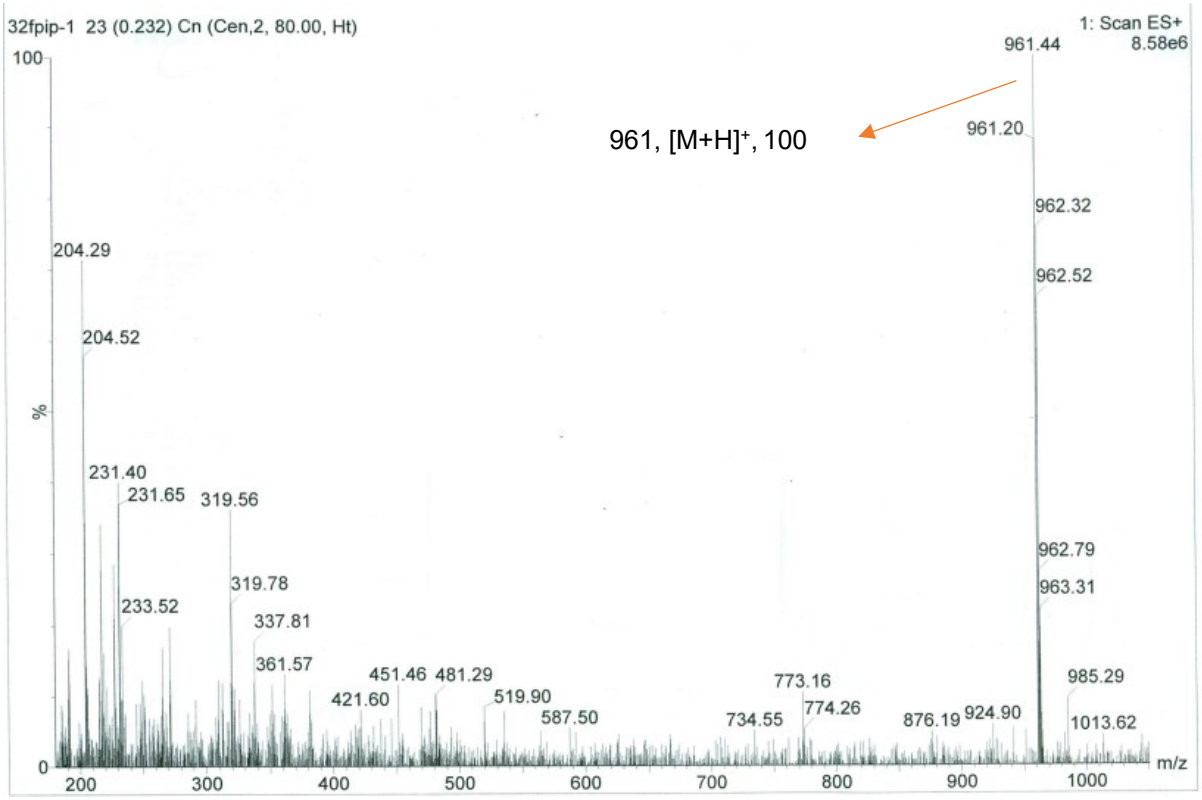


ESI-MS spectra of compounds **1b**.

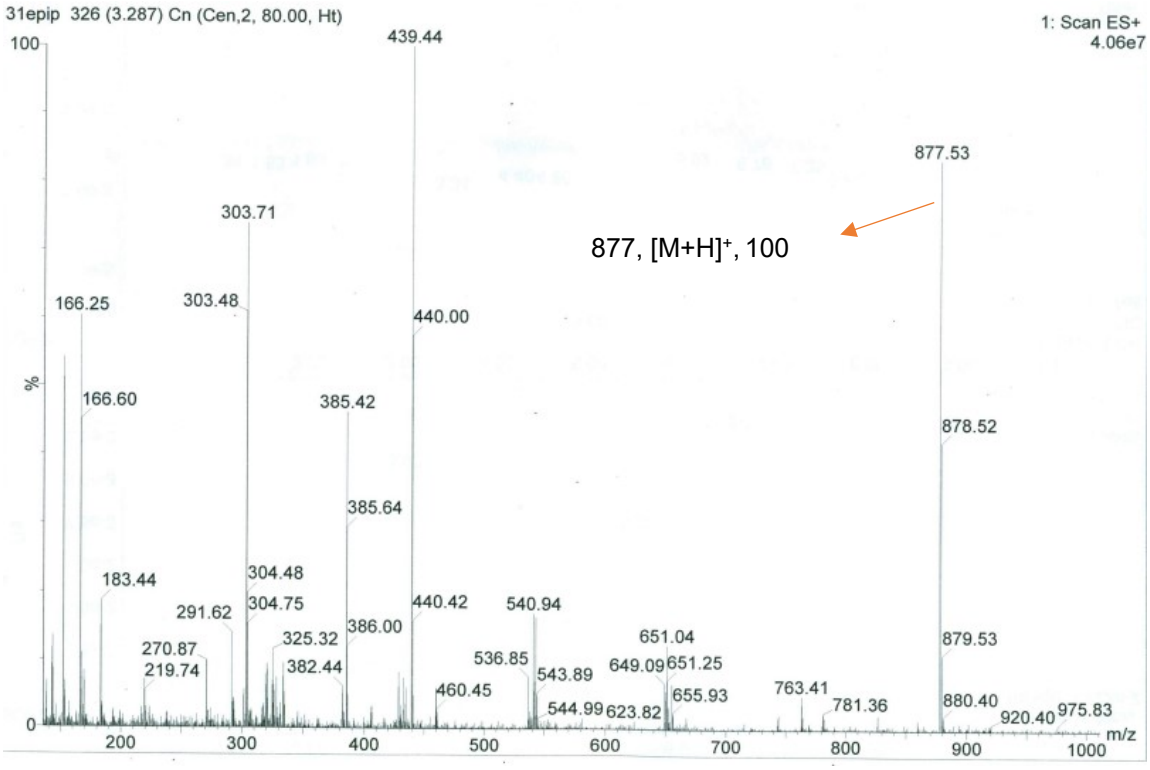


ESI-MS spectra of compounds **2a**.

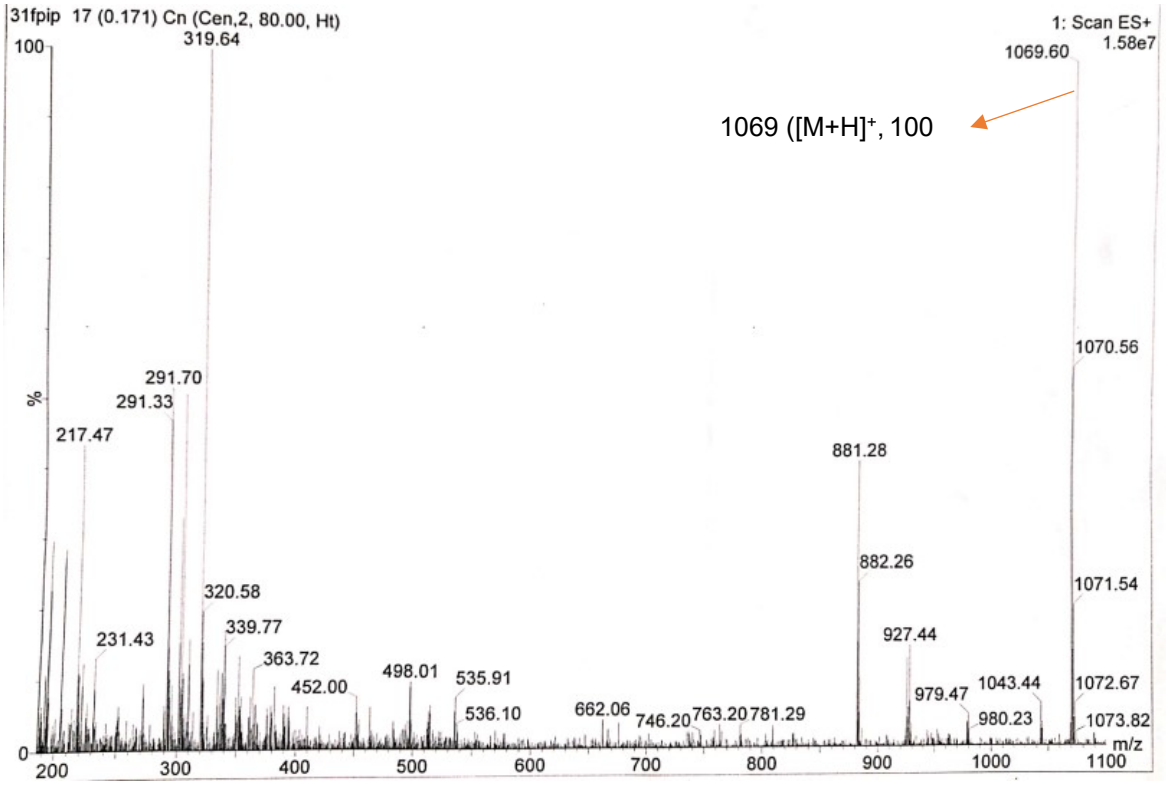

ESI-MS spectra of compounds **2b**.

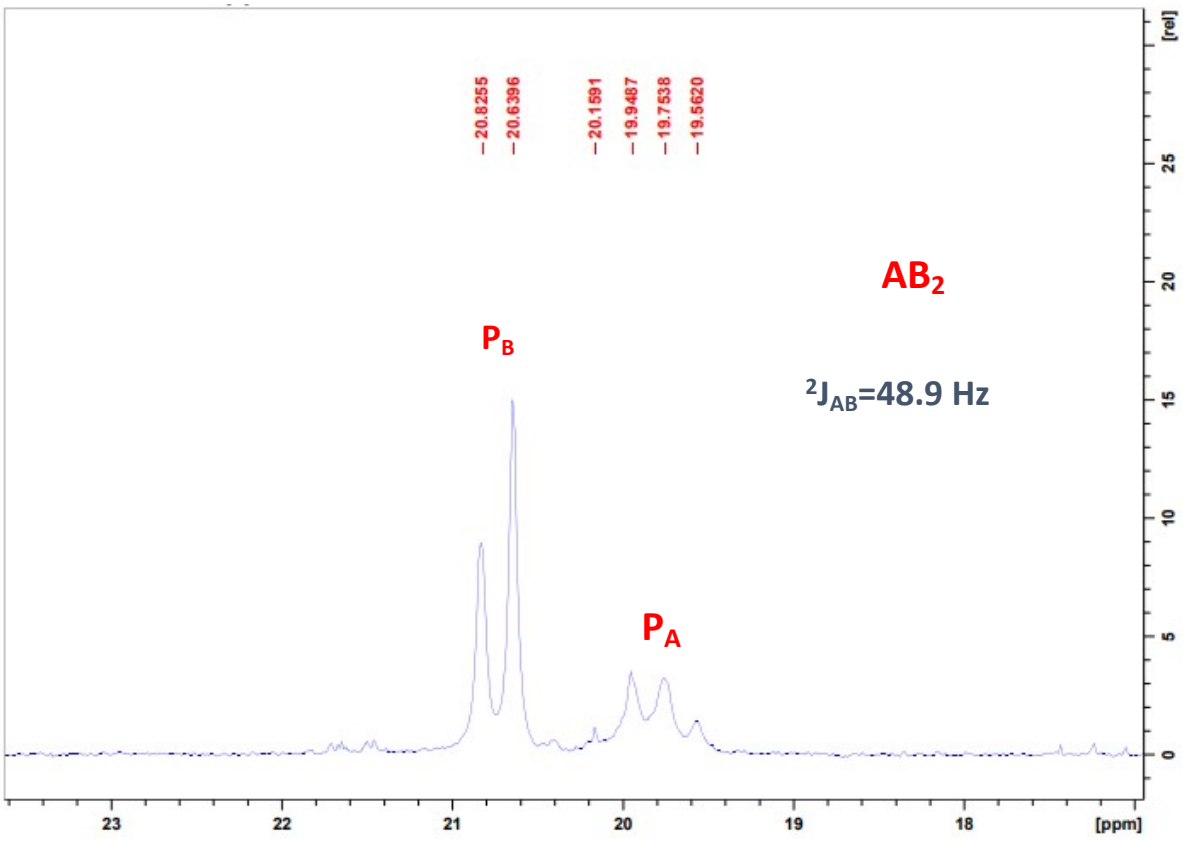


$^{31}$P NMR spectrum of compound **1a.**

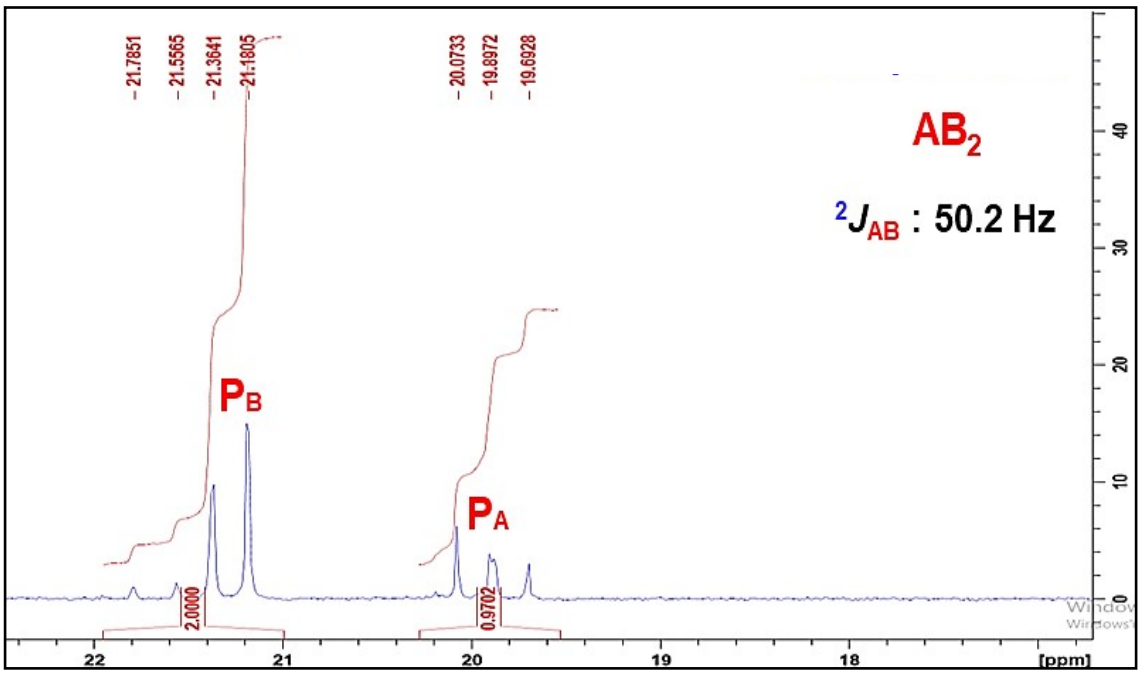


$^{31}$P NMR spectrum of compound **1b.**

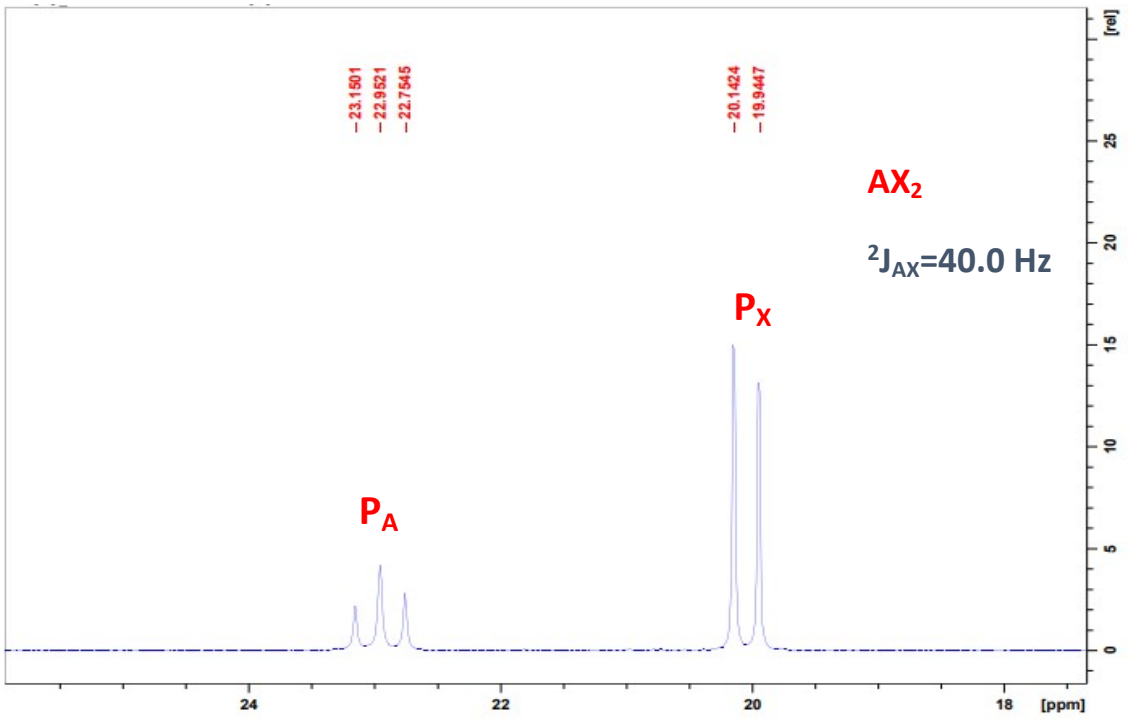


$^{31}$P NMR spectrum of compound **2a.**

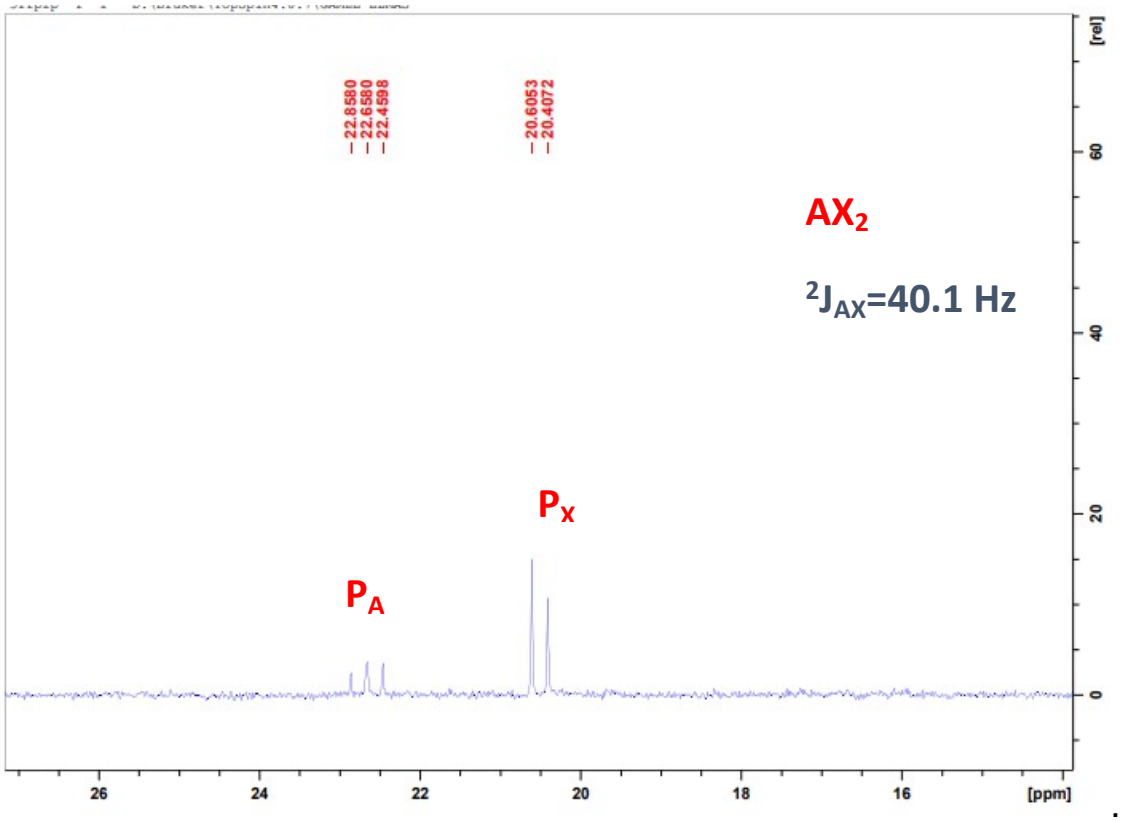


$^{31}$P NMR spectrum of compound **2b.**

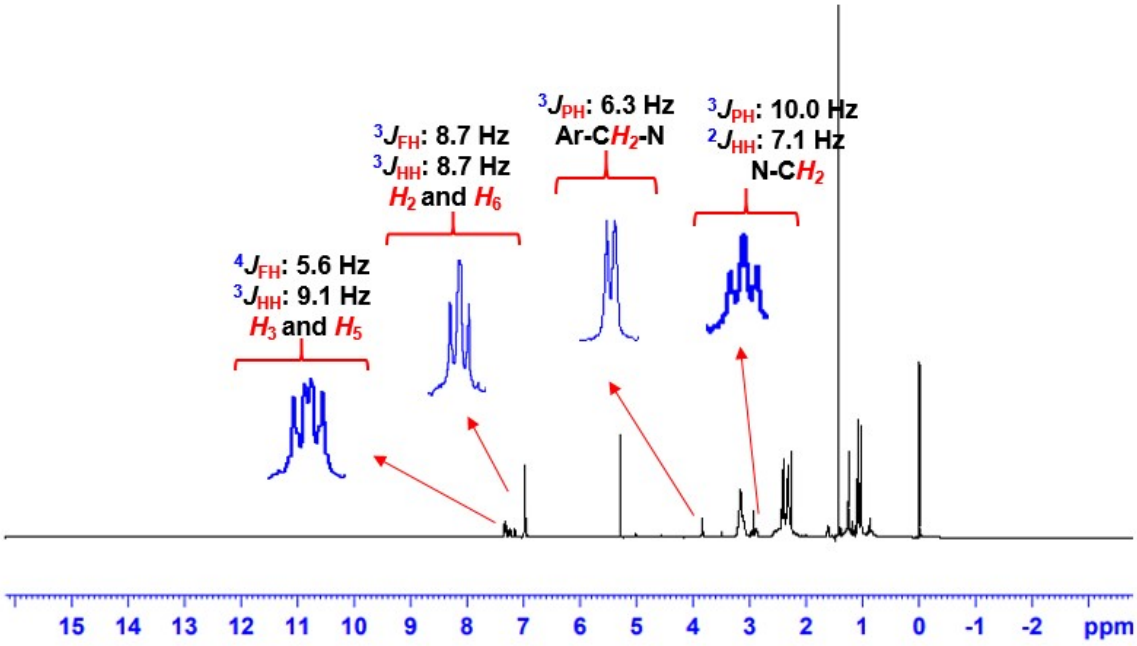


$^{1}$H NMR spectrum of compound **1a.**

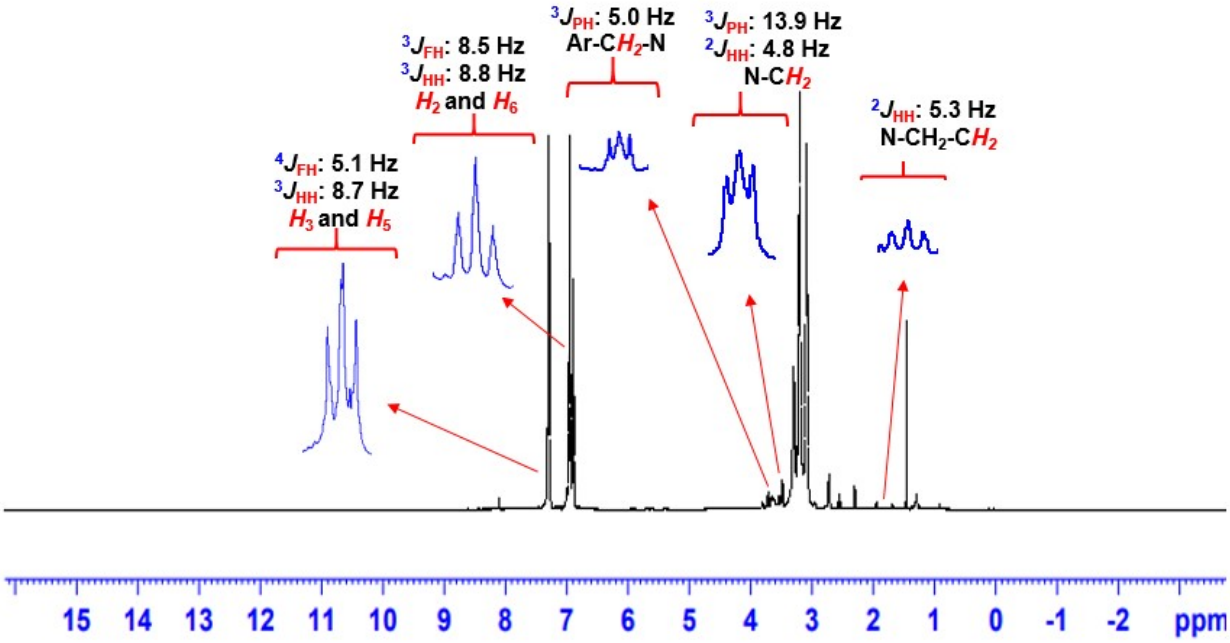


$^{1}$H NMR spectrum of compound **1b.**

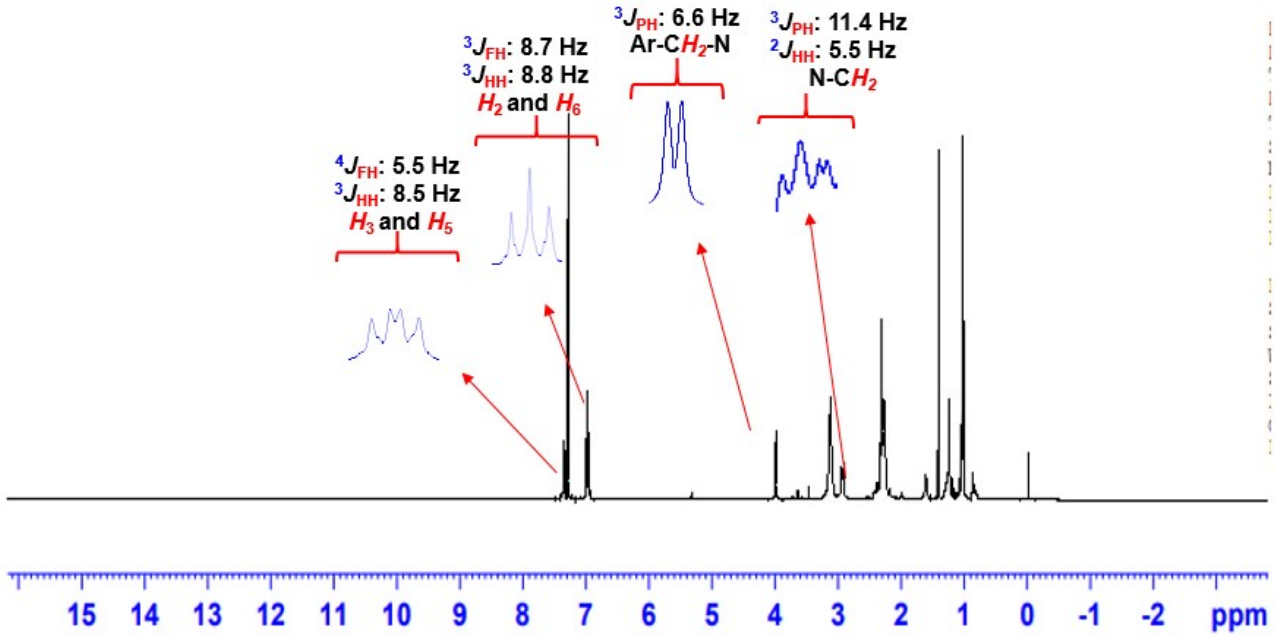


$^{1}$H NMR spectrum of compound **2a.**

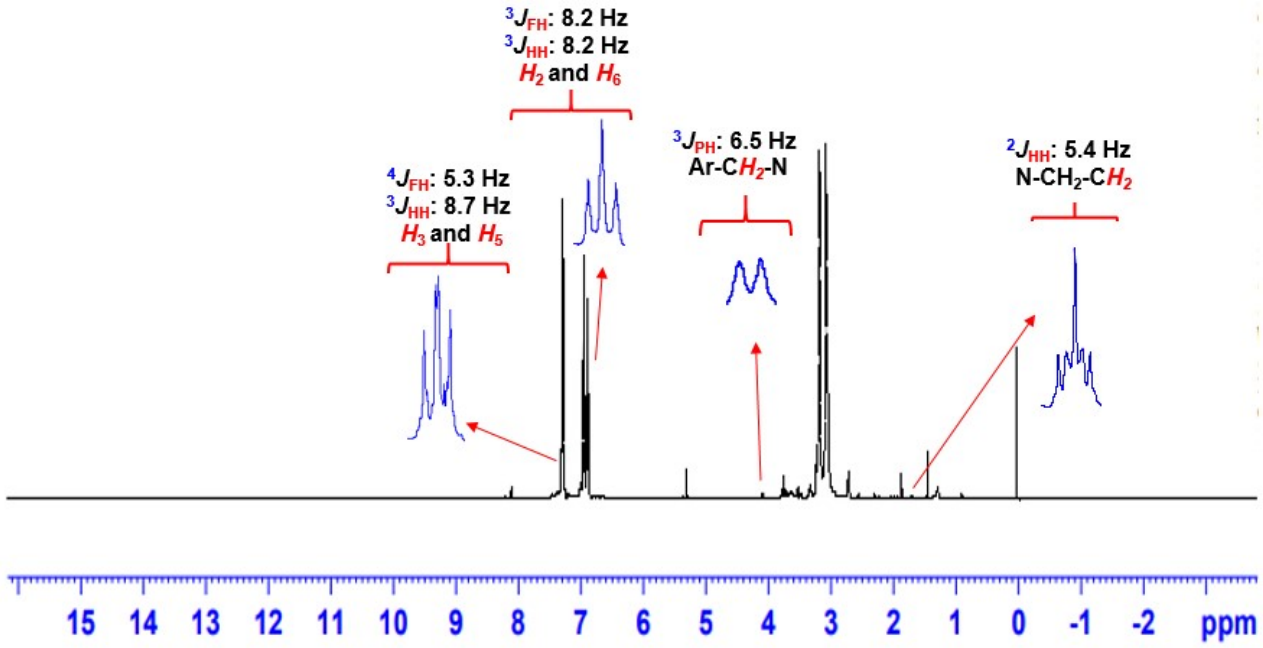


$^{1}$H NMR spectrum of compound **2b.**

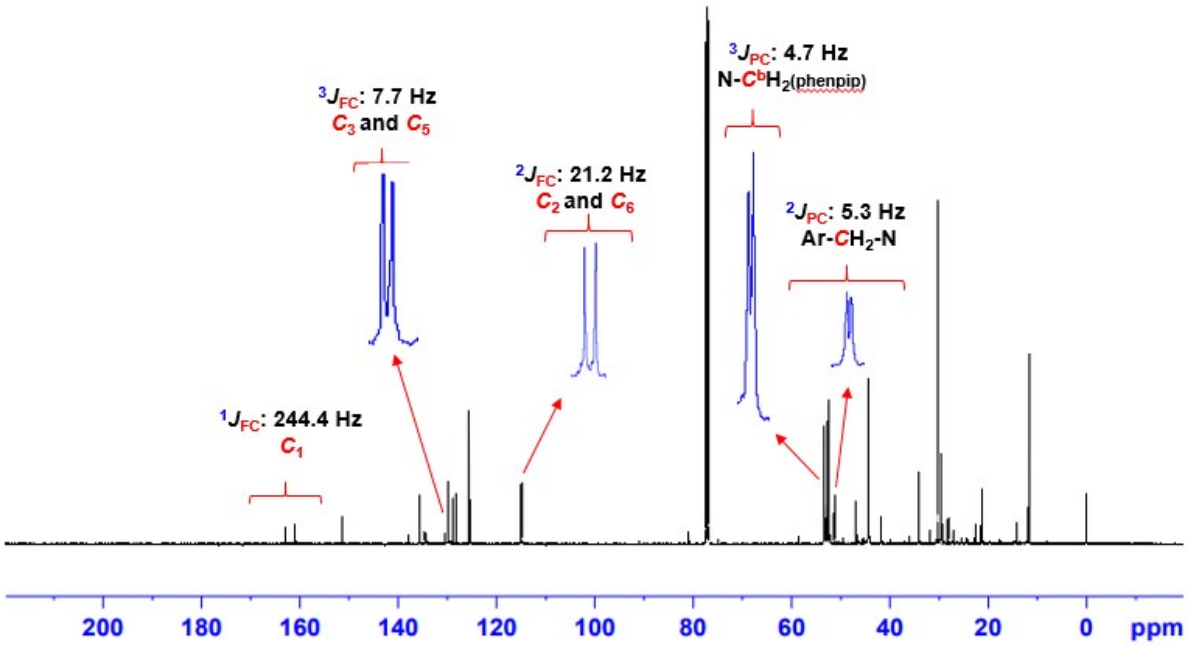


$^{13}$C NMR spectrum of compound **1a.**

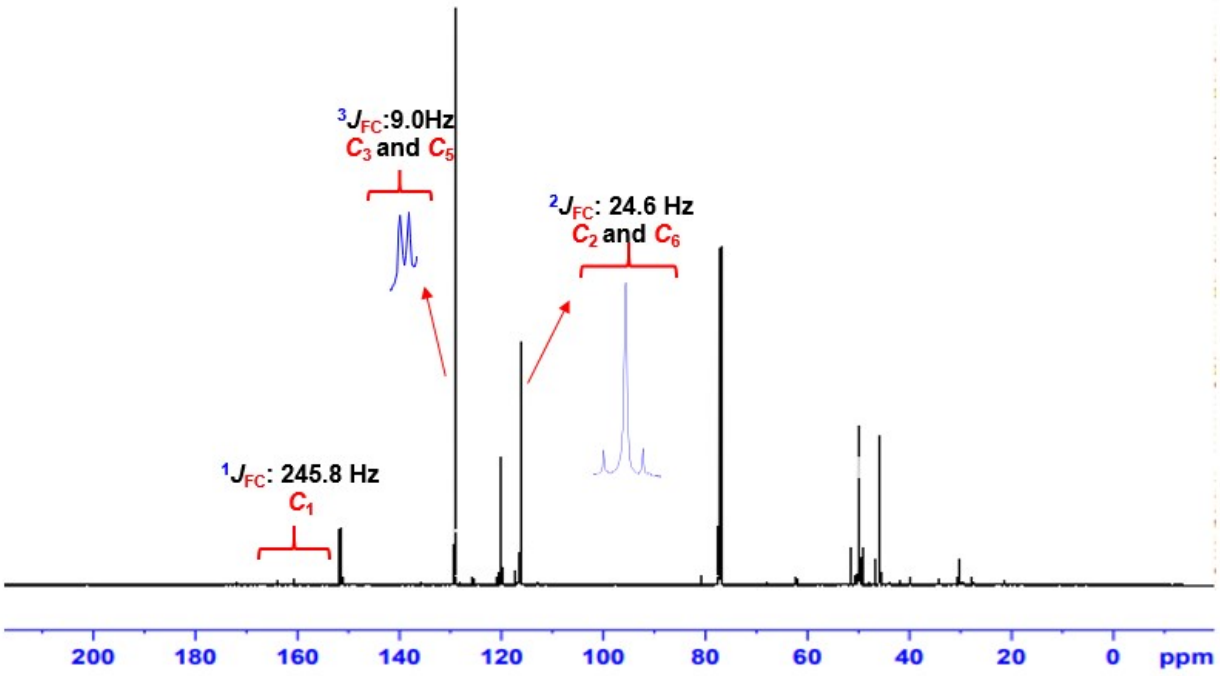


$^{13}$C NMR spectrum of compound **1b.**

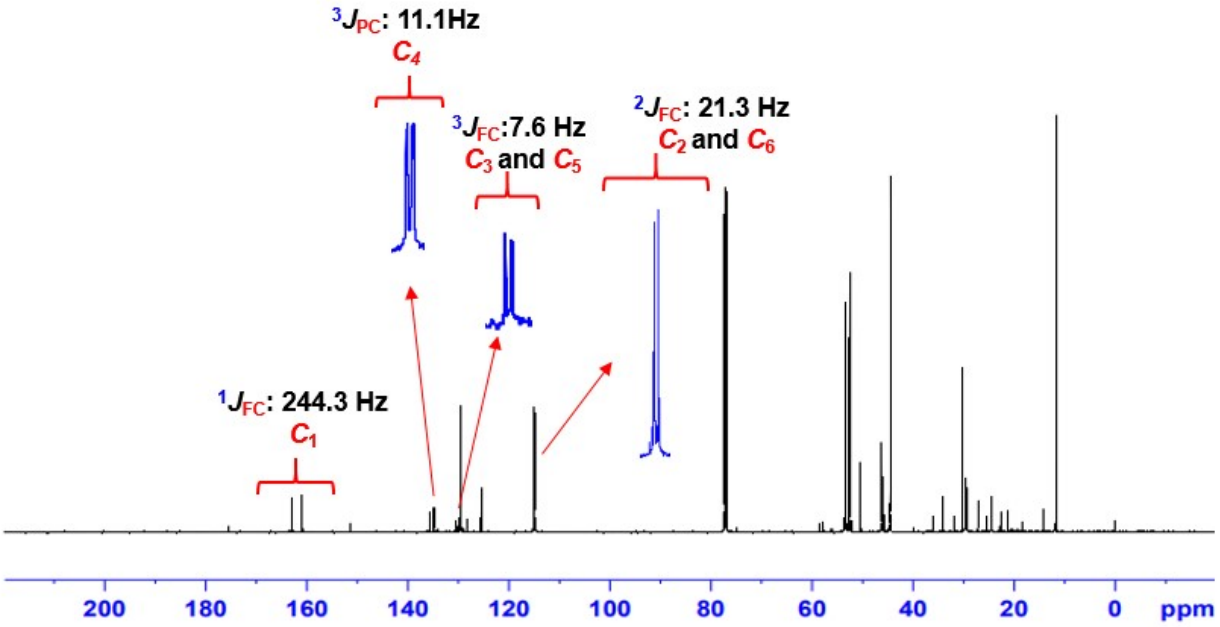


$^{13}$C NMR spectrum of compound **2a.**

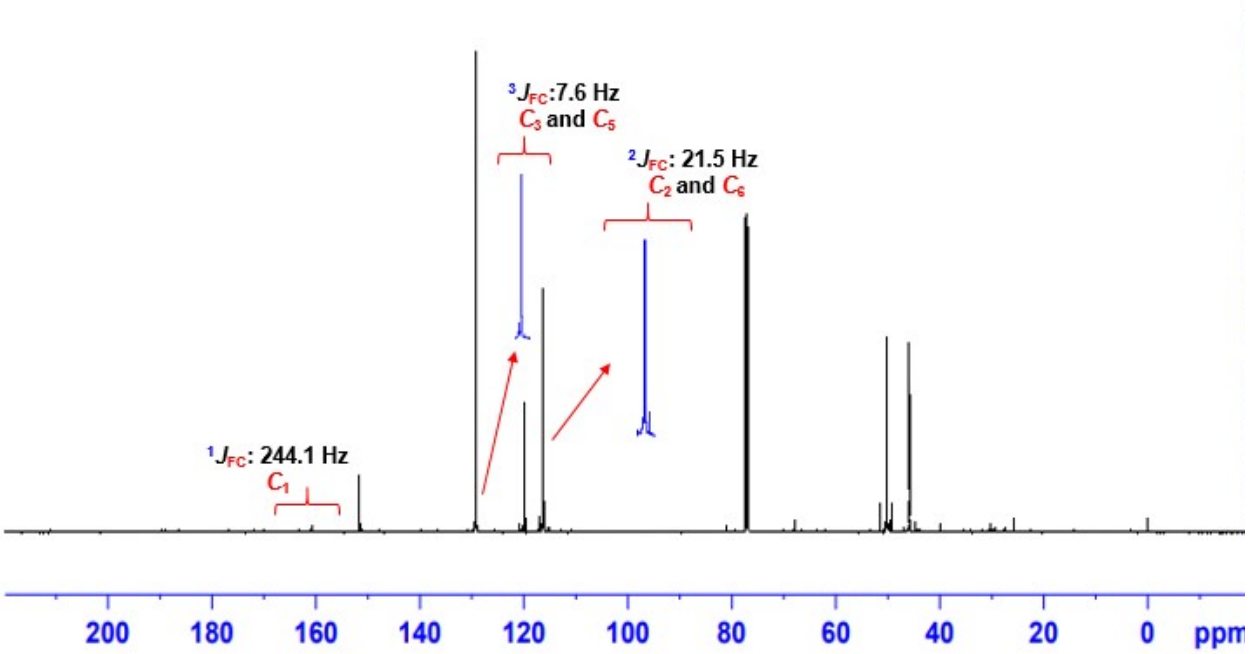


$^{13}$C NMR spectrum of compound **2b.**

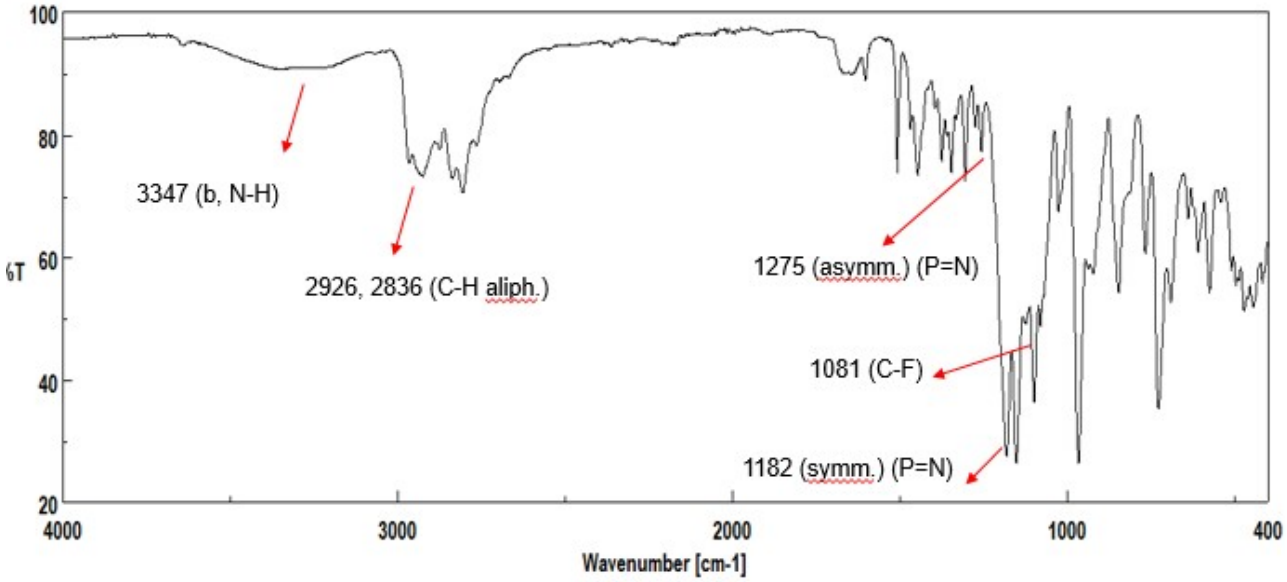


IR spectrum of compound **1a.**

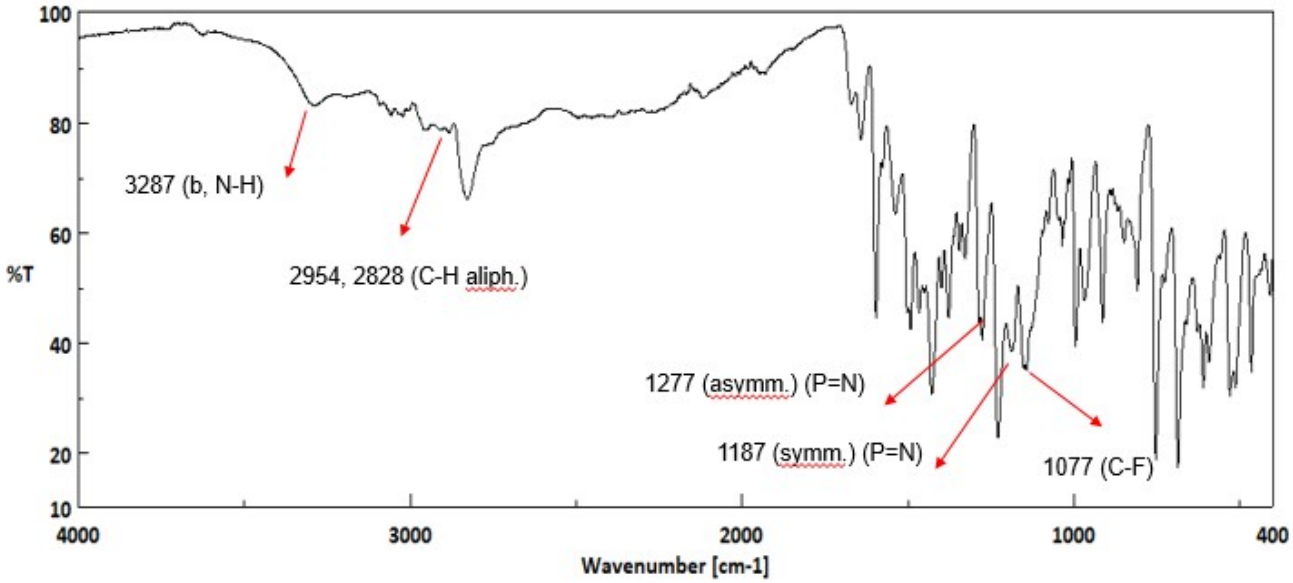


IR spectrum of compound **1b.**

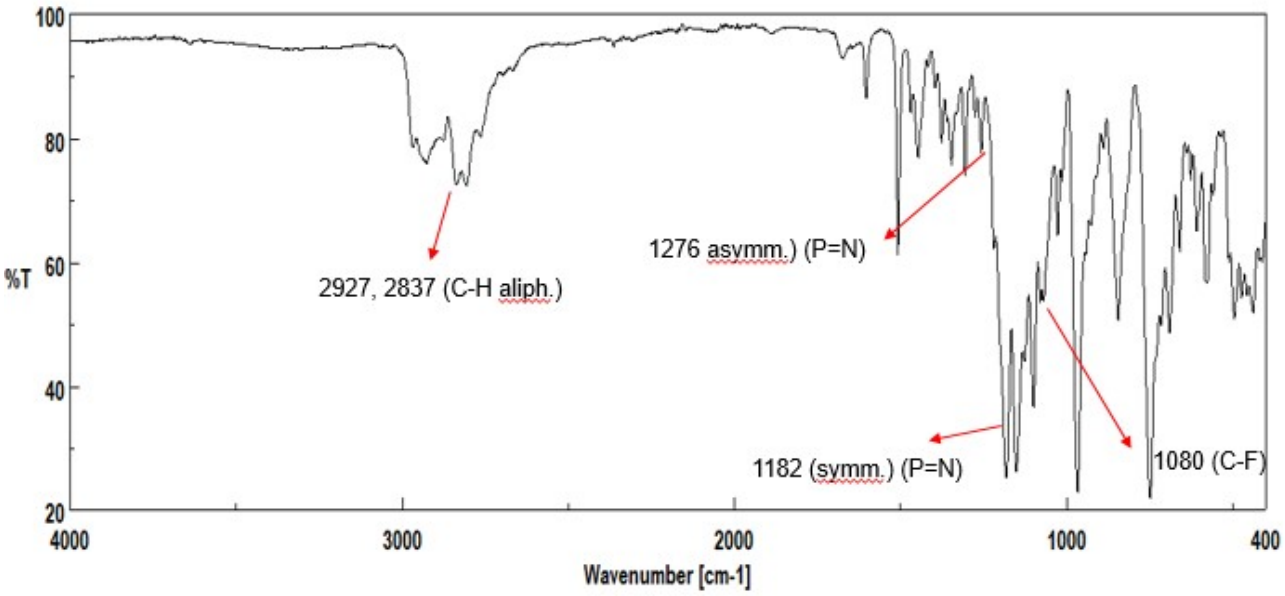


IR spectrum of compound **2a.**

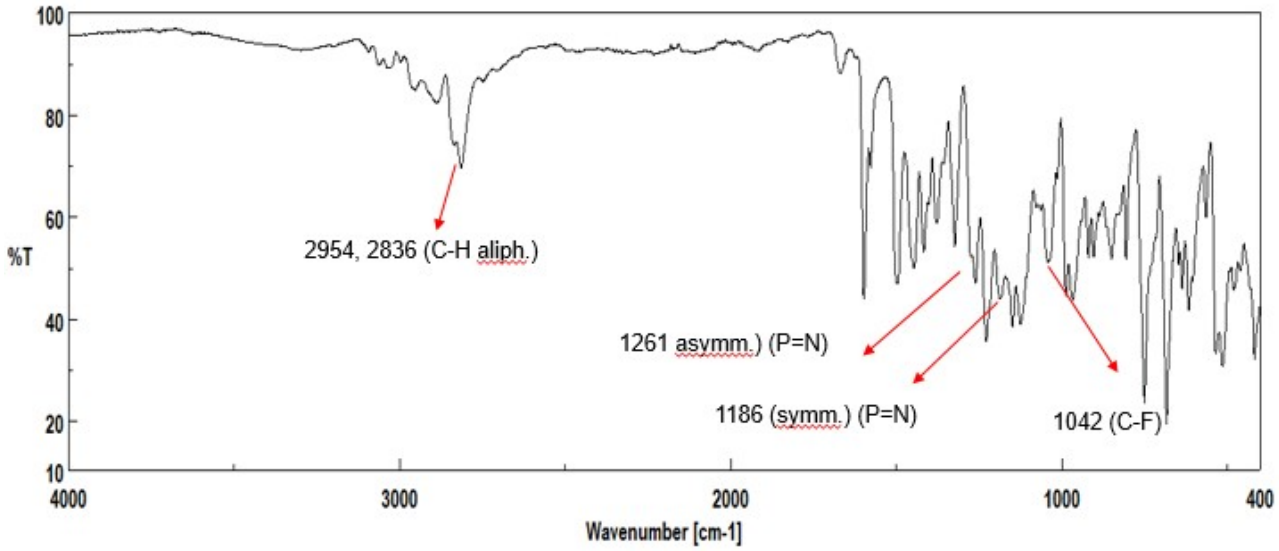


IR spectrum of compound **2b.**

## Section S2. Determination of *in vitro* inhibitory activity

### *i. Purification of carbonic anhydrase I and II isoenzymes from human erythrocytes*

The hCA I and hCA II isoenzymes were purified from human erythrocytes according to our previous studies in the literature. Briefly, the blood samples were centrifuged and the plasma was removed. Later, red cells were washed with an isotonic solution (0.9% NaCl), and the erythrocytes were hemolyzed with ice-cold water. Cell membranes were removed by centrifugation at 4 °C at 20000 rpm for 30 minutes. Hemolysate was applied to affinity column (Sepharose®4B-L-tyrosine-*p*-aminobenzene sulfonamide). After extensive washing, the hCA I and hCA II isoenzymes were eluted with the solution of 1.0 M NaCl/25.0 mM $Na_2HPO_4$ (pH 6.3) and 0.1 M $NaCH_3COO$/0.5 M $NaClO_4$ (pH 5.6), respectively.[1] For quantitative protein determination, the Bradford method was used with bovine serum albumin as standard.[2] Also, the purity control of the isoenzymes was performed with SDS-PAGE after the purification.[3]

### *ii. Determination of esterase activities of hCA I and hCA II*

Esterase activity was examined by following the change in the absorbance at 348 nm of 4-nitrophenyl acetate to 4-nitrophenolate ion over a period of 3 min at 25 °C using a spectrophotometer according to the method described in the literature.[4,5]

### *iii. Determination of $IC_{50}$ and $K_i$ values of the compounds*

To determine the $IC_{50}$ values (the concentration of inhibitor producing a 50% inhibition of CA activity) of the compounds, the esterase activities of CA isoenzymes were examined in the presence of various inhibitor concentrations. Regression analysis graphs were drawn by plotting the percent enzyme activity versus inhibitor concentration and $IC_{50}$ values were calculated.[6,7]

To determine the $K_i$ values as well as the inhibition type, three different inhibitor concentrations giving 30%, 50%, and 70% inhibition were selected. For each inhibitor concentrations, enzyme activity was measured in the presence of various substrate concentrations (0.3 mM, 0.4 mM, 0.5 mM, 0.6 mM and 0.7 mM) and the data were linearized with Lineweaver–Burk plot for $V_{max}$ and the $K_i$ determination. Enzyme activity was also measured in the presence of the same substrate concentrations but in the absence of any inhibitor to determine the $V_{max.}$[6,7]

### *iv. Statistical analysis*

All the presented data were confirmed with three independent experiments and were expressed as the mean ± standard deviation (SD). Data were analyzed by using a one-way analysis of variance for multiple comparisons (SPSS 13.0, SPSS Inc., Chicago, IL). $p < 0.0001$ was considered to be statistically significant.

**References**

[1] Rickli E. E., Ghazanfar S. A. S., Gibbons B. H., Edsall J. T., Carbonic anhydrases from human erythrocytes. Preparation and properties of two enzymes, *Journal of Biological Chemistry*, **1964**, *239*, 1065-1078.

[2] Bradford M. M., A rapid and sensitive method for the quantitation of microgram quantities of protein utilizing the principle of protein-dye binding, *Analytical Biochemistry*, **1976**, *72*, 248-254.

[3] Laemmli U. K., Cleavage of structural proteins during the assembly of the head of bacteriophage T4, *Nature*, **1970**, *227*, 680-685.

[4] Verpoorte J. A., Mehta S., Edsall J. T., Esterase activities of human carbonic anhydrases B and C, *Journal of Biological Chemistry*, **1967**, *242*, 4221-4429.

[5] Alkan Alkaya Z., İlkimen H., Yenikaya C., Tunca E., Bülbül M., Tunç T., Sarı M., Synthesis and characterization of Cu(II) complexes of 2-amino-6-sulfamoylbenzothiazole and their inhibition studies on carbonic anhydrase isoenzymes, *Polyhedron*, **2018**, *151*, 199-205.

[6] Yenikaya C., İlkimen H., Demirel M. M., Ceyhan B., Bülbül M., Tunca E., Preparation of two maleic acid sulfonamide salts and their copper(II) comolexes and antiglaucoma activity studies, *Journal of the Brazilian Chemical Society*, **2016**, *27(10)*, 1706-1714.

[7] Mert S., Alım Z., İşgör M. M., Anıl B., Kasımoğulları R., Beydemir Ş., Novel pyrazole-3,4-dicarboxamides bearing biologically active sulfonamide moiety as potential carbonic anhydrase inhibitors, Arabian Journal of Chemistry, **201**9, *12(8),* 2740-2748.

**Table S1.** Selected Calculated Bond Lengths (Å) and Angles (deg) for **2b**

| | **2b** | | **2b** |
|---|---|---|---|
| P1– N3 | 1.599(2) | N1– P2– N2 | 117.38(11) |
| P1– N1 | 1.586(2) | N1– P1– N3 | 115.32(10) |
| P1– N5 | 1.682(2) | N1– P1– N4 | 108.30(10) |
| P2– N2 | 1.590(2) | N3– P1– N4 | 110.86(11) |
| P2– N1 | 1.599(2) | N1– P1– N5 | 109.05(10) |
| P2– N8 | 1.667(2) | P1– N1– P2 | 122.36(12) |
| P1– N4 | 1.663(2) | P2– N2– P3 | 122.64(13) |
| P2– N6 | 1.647(2) | N2– P3– N3 | 116.07(10) |
| P3– N2 | 1.591(2) | N4– P1– N5 | 101.83(10) |
| P3– N3 | 1.594(2) | N10– P3– N12 | 100.08(11) |
| P3– N12 | 1.647(2) | N5– P1– N3 | 110.61(10) |
| P3– N10 | 1.654(2) | P1– N3– P3 | 122.52(12) |

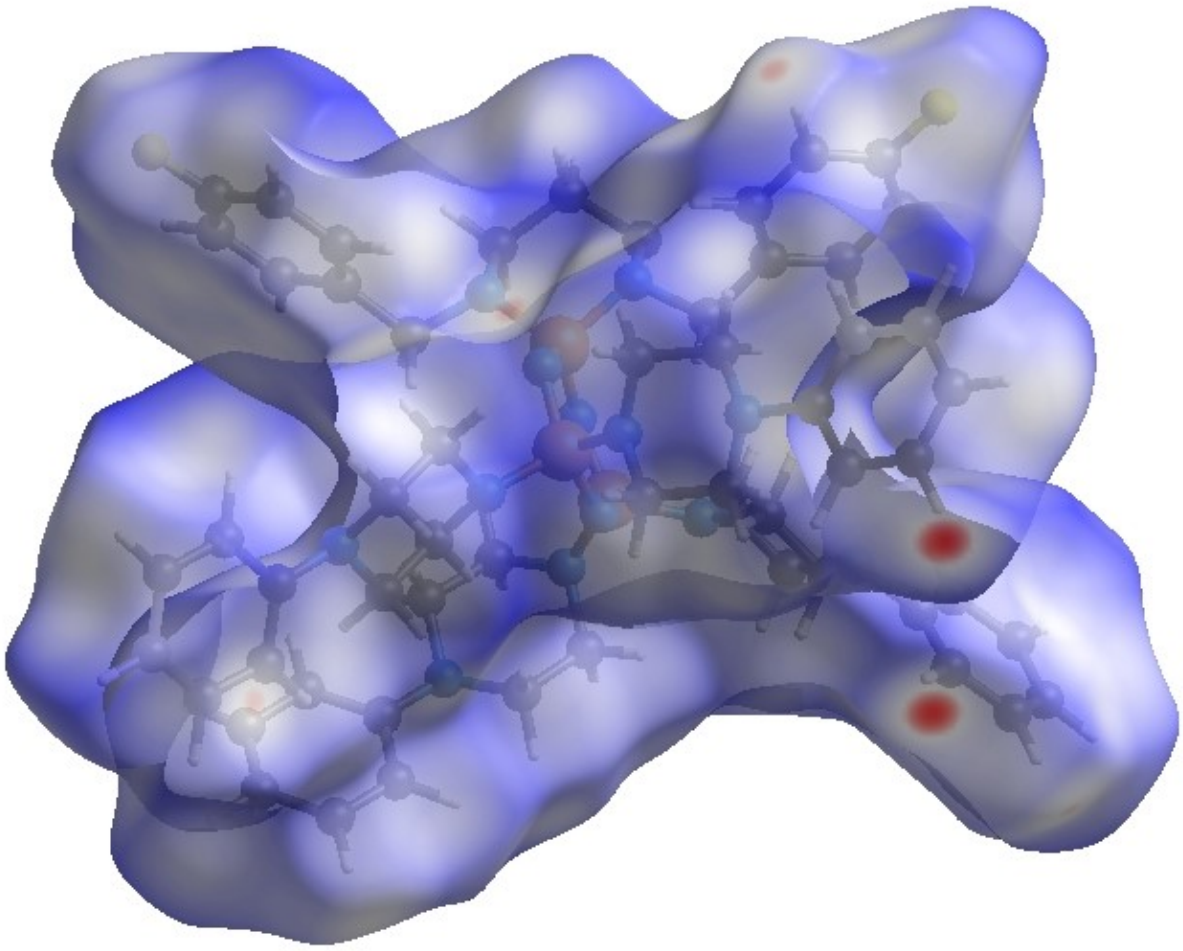

**Figure S1.** View of the three-dimensional Hirshfeld surface of the title compound plotted over $d_{norm}$.

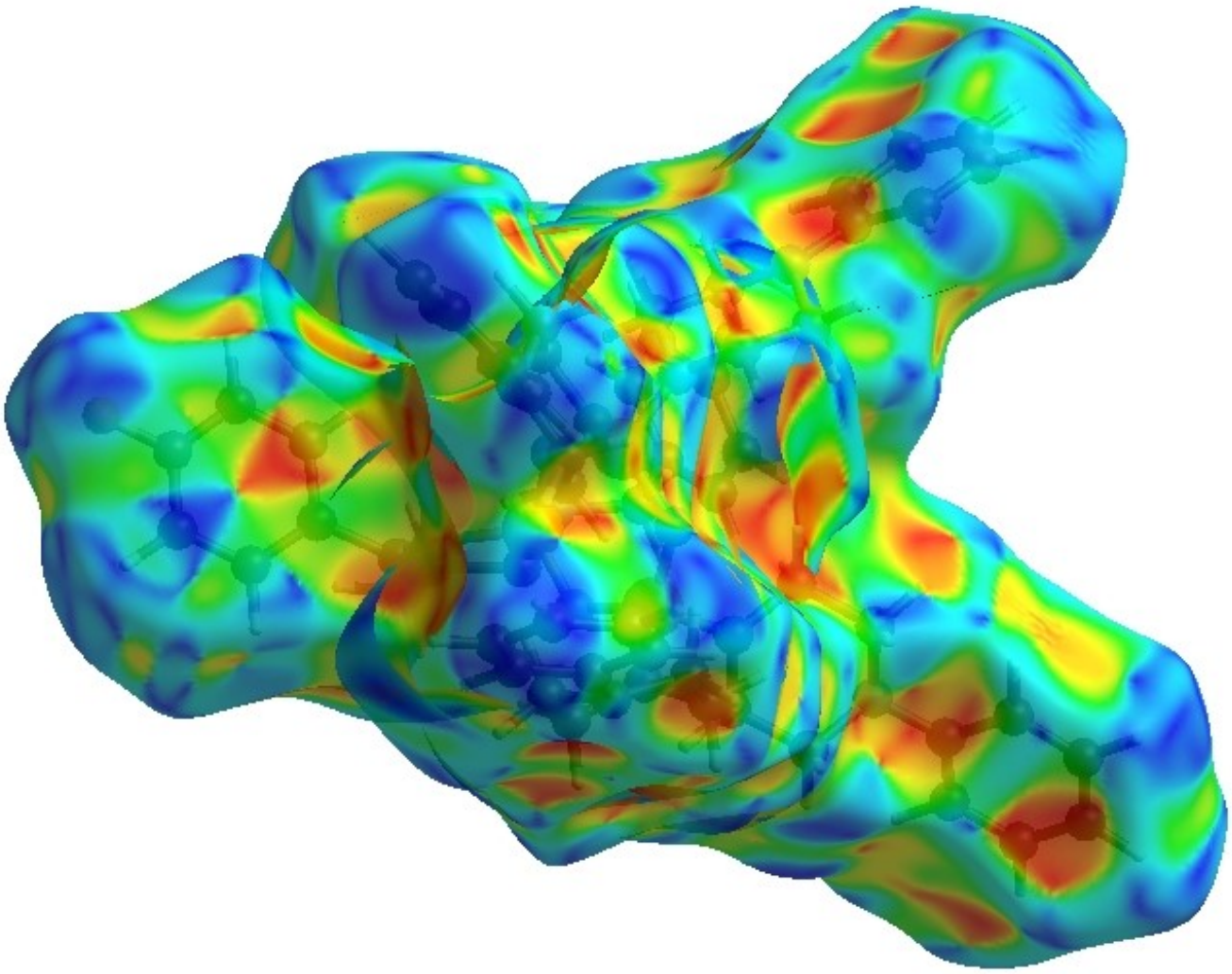

**Figure S2.** Hirshfeld surface of the title compound plotted over shape-index.

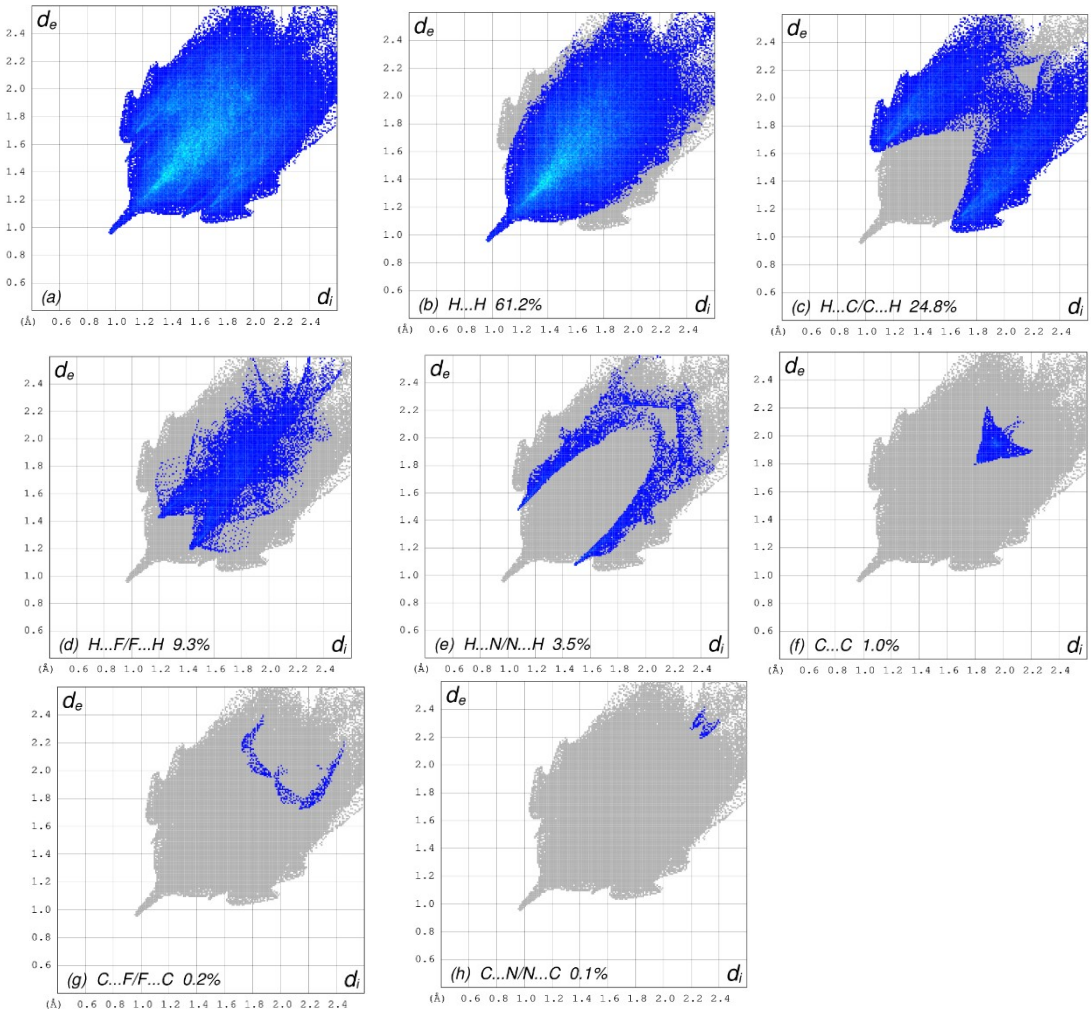


**Figure S3.** The full two-dimensional fingerprint plots for the title compound, showing (a) all interactions, and delineated into (b) H ... H, (c) H ... C/C ... H, (d) H ... F/F ... H, (e) H ... N/N … H, (f) C ... C, (g) C ... F/F ... C and (h) C … N/N … C interactions. The $d_i$ and $d_e$ values are the closest internal and external distances (in Å) from given points on the Hirshfeld surface contacts.

**Table S2** Selected interatomic distances (Å)

| | | | |
|---|---|---|---|
| N1···H14$^{i}$ | 2.70 | C37···H31A | 2.66 |
| N1···H11B | 2.73 | C39···H43 | 2.48 |
| N1···H18B | 2.48 | C40···H47 | 2.81 |
| N1···H7A | 2.70 | C43···H39A | 2.67 |
| N2···H30A | 2.53 | C43···H39B | 2.82 |
| N2···H38A | 2.54 | C47···H40B | 2.61 |
| N3···H48B | 2.50 | C49···H53 | 2.47 |
| N6···H28B | 2.71 | C50···H57 | 2.49 |
| N10···H51A | 2.60 | C53···H49A | 2.78 |
| N12···H41B | 2.61 | C53···H49B | 2.63 |
| C3···F2$^{i}$ | 3.299 (4) | C56···H21A$^{v}$ | 2.86 |
| C1···H24$^{i}$ | 2.86 | C57···H50A | 2.61 |
| C2···H24$^{i}$ | 2.78 | C57···H50B | 2.82 |
| C4···H8A | 2.76 | H5···H7B | 2.37 |
| C11···H38B | 2.88 | H10A···H11A | 2.39 |
| C12···H10B | 2.68 | H11A···H17 | 2.33 |
| C16···H9A$^{ii}$ | 2.89 | H20A···H27 | 1.99 |
| C17···H44$^{iii}$ | 2.88 | H26···H43$^{vi}$ | 2.17 |
| C19···H23 | 2.51 | H29B···H33 | 2.20 |
| C20···H27 | 2.63 | H30A···H49A | 2.26 |
| C23···H19B | 2.56 | H30A···H50B | 2.24 |
| C27···H20A | 2.53 | H31A···H37 | 2.23 |
| C27···H17$^{iv}$ | 2.89 | H31B···H37 | 2.39 |
| C29···H33 | 2.79 | H39A···H43 | 2.20 |
| C30···H49A | 2.75 | H39B···H43 | 2.33 |
| C31···H37 | 2.52 | H40B···H47 | 2.23 |
| C33···H29B | 2.61 | H49B···H53 | 2.06 |
| C36···H49B$^{iv}$ | 2.83 | H50A···H57 | 2.05 |
| C37···H31B | 2.87 | | |

Symmetry codes: (i) −x, −y+1, −z+1; (ii) −x+1, −y+1, −z+1; (iii) −x+1, −y+1, −z; (iv) x−1, y, z; (v) −x, −y+2, −z; (vi) −x, −y+1, −z.

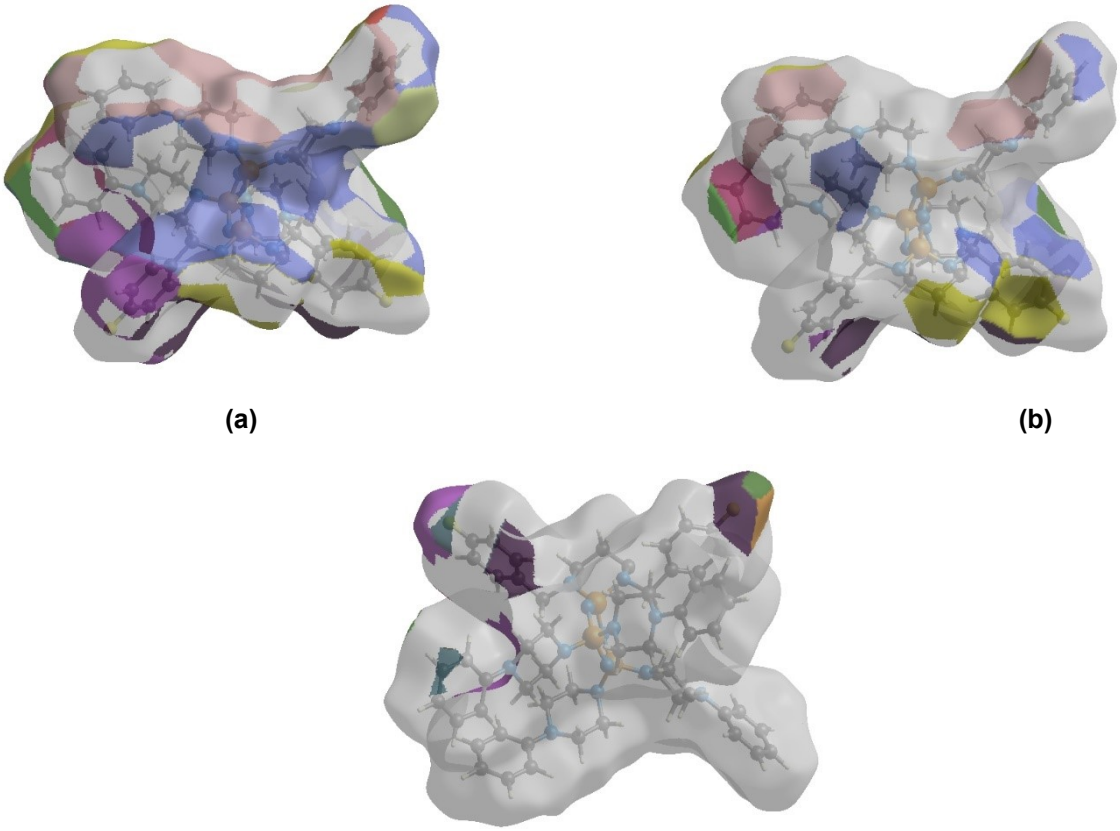

**(a)** **(b)**

**(c)**

**Figure S4.** The Hirshfeld surface representations with the function $d_{norm}$ plotted onto the surface for (a) H ... H, (b) H ... C/C ... H and (c) H ... F/F ... H interactions.

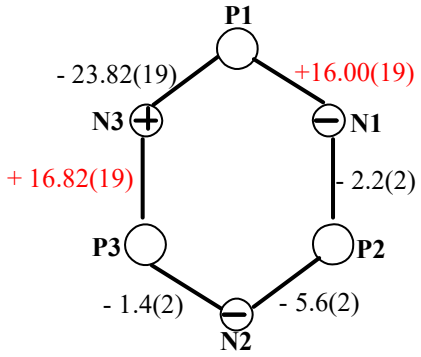


**Figure S5.** The shape of the phosphazene ring in **2b** with torsion angles (deg) given.


**(a)**

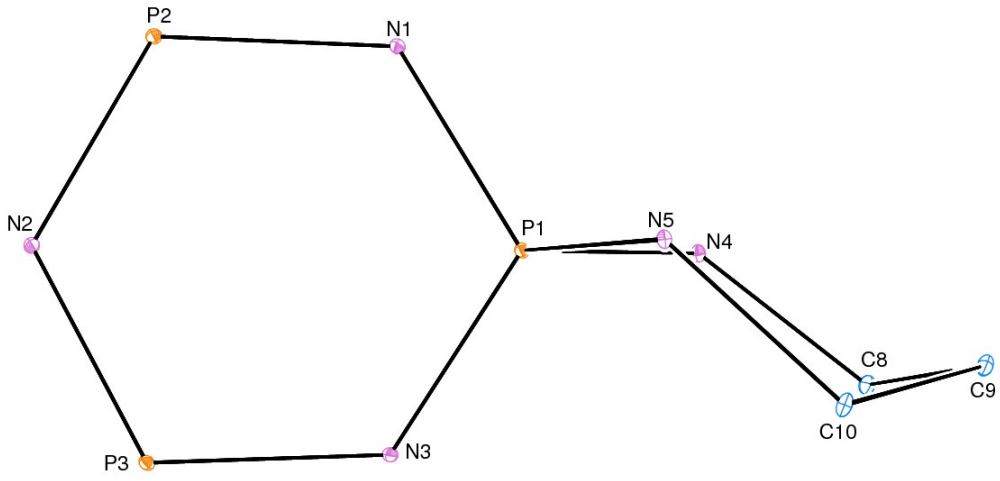


**(b)**

**Figure S6.** The conformations of (**a**) the trimer ring and (**b**) the spiro ring of **2b.**

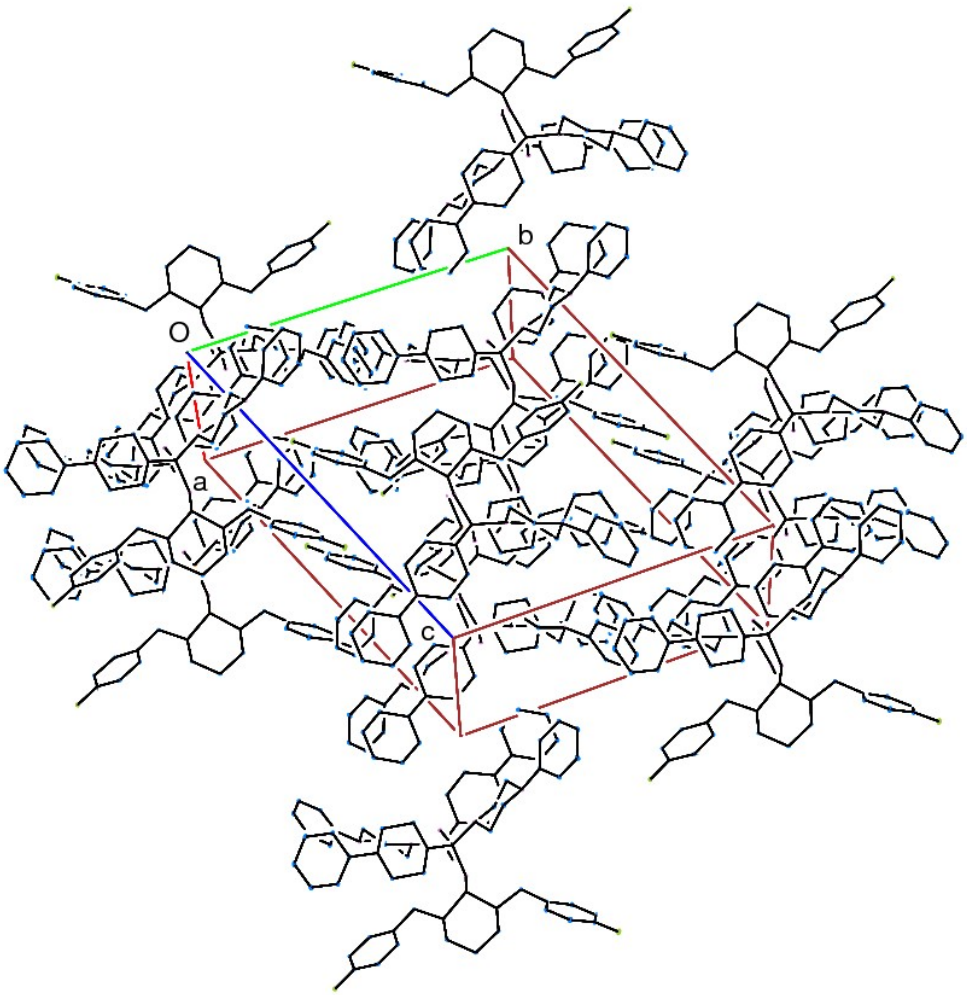


**Figure S7.** The packing diagram of **2b.**